ARTICLE

Cyclin B2 can compensate for Cyclin B1 in oocyte meiosis I

Jian Li[1,2]*, Ji-Xin Tang[1]*, Jin-Mei Cheng[1], Bian Hu[3,4], Yu-Qian Wang[1,5], Batool Aalia[1,5], Xiao-Yu Li[1,5], Cheng Jin[1], Xiu-Xia Wang[1], Shou-Long Deng[1], Yan Zhang[1], Su-Ren Chen[1], Wei-Ping Qian[2], Qing-Yuan Sun[1,5], Xing-Xu Huang[3,4], and Yi-Xun Liu[1,5]

Mammalian oocytes are arrested at the prophase of the first meiotic division for months and even years, depending on species. Meiotic resumption of fully grown oocytes requires activation of M-phase–promoting factor (MPF), which is composed of Cyclin B1 and cyclin-dependent kinase 1 (CDK1). It has long been believed that Cyclin B1 synthesis/ accumulation and its interaction with CDK1 is a prerequisite for MPF activation in oocytes. In this study, we revealed that oocyte meiotic resumption occurred in the absence of Cyclin B1. *Ccnb1*-null oocytes resumed meiosis and extruded the first polar body. Without Cyclin B1, CDK1 could be activated by up-regulated Cyclin B2. *Ccnb1* and *Ccnb2* double knockout permanently arrested the oocytes at the prophase of the first meiotic division. Oocyte-specific *Ccnb1*-null female mice were infertile due to failed MPF activity elevation and thus premature interphase-like stage entry in the second meiotic division. These results have revealed a hidden compensatory mechanism between Cyclin B1 and Cyclin B2 in regulating MPF and oocyte meiotic resumption.

Introduction

At birth, mammalian oocytes are arrested at the first meiotic prophase, characterized by the presence of a germinal vesicle (GV). The resumption of meiosis as characterized by GV breakdown (GVBD) only occurs after puberty following stimulation via luteinizing hormone or release of fully-grown oocytes from antral follicles (Borum, 1961; Adhikari et al., 2012; Polański et al., 2012; Adhikari and Liu, 2014). The meiotic prophase arrest results from low M-phase–promoting factor (MPF), which is a complex of Cyclin B1 and cyclin-dependent kinase 1 (CDK1; Draetta et al., 1989; Labbé et al., 1989; Gautier et al., 1990; Jones, 2004; Adhikari and Liu, 2014). Two pathways are involved in maintenance of prophase I arrest in the fully grown oocytes. One is the protein kinase A (PKA) phosphorylation pathway, which is activated by cAMP contributed by both cumulus cells and oocyte itself through activation of G-protein–coupled membrane receptor (Norris et al., 2007) as well as PDE3 inhibition by cGMP contributed by cumulus cells (Zhang et al., 2010). Subsequently, high PKA activity stimulates WEE1B kinase activity, which ensures inhibitory phosphorylation on threonine 14 and tyrosine 15 of CDK1 and inhibits the activity of CDC25B, which keeps low MPF activity. The other pathway is APC/C[cdh1] ubiquitylation/degradation pathway, which prevents the MPF activation by reduced Cy-clin B1 accumulation (Reis et al., 2006). To establish the threshold of MPF activity that is capable of promoting GVBD in addition to preventing WEE1/MYT kinase family–mediated inhibitory phosphorylation on CDK1 (also commonly known as p34cdc2 or CDC2) by CDC25 phosphatases (Han et al., 2005; Solc et al., 2010), it also requires a sufficient accumulation of Cyclin B1 (Dorée and Hunt, 2002; Polański et al., 2012). In mice, unlike in other species, the dephosphorylation of inactive Cyclin B1–CDK1 complex preformed during oocyte growth is sufficient for inducing GVBD (Choi et al., 1991; Polanski et al., 1998; Ledan et al., 2001; Polański et al., 2012). Moreover, the translocation of Cyclin B1 from the cytoplasm into the nucleus before GVBD in GV-intact oocytes is an important step to bring about GVBD (Clute and Pines, 1999; Marangos and Carroll, 2004; Reis et al., 2006; Holt et al., 2010).

In mammals, three B-type cyclins exist: Cyclin B1, Cyclin B2, and Cyclin B3. Cyclin B3 associates with CDK2, while the other two cyclins associate with CDK1 (Nguyen et al., 2002; Satyanarayana and Kaldis, 2009). However, it is mainly Cyclin B1 that combines with CDK1 to activate MPF in meiotic oocytes (Homer, 2013; Polánski et al., 2012; Porter and Donoghue, 2003; Satyanarayana and Kaldis, 2009). Cyclin B1 and Cyclin B2 knockout mice have been generated (Brandeis et al., 1998),

[1]State Key Laboratory of Stem Cell and Reproductive Biology, Institute of Zoology, Chinese Academy of Sciences, Beijing, China;   [2]Department of Reproductive Medicine, Peking University Shenzhen Hospital, Shenzhen Peking University–The Hong Kong University of Science and Technology Medical Center, Shenzhen, China;   [3]School of Life Science and Technology, Shanghai Tech University, Shanghai, China;   [4]Ministry of Education Key Laboratory of Model Animal for Disease Study, Model Animal Research Center of Nanjing University, Nanjing, China;   [5]University of Chinese Academy of Sciences, Beijing, China.

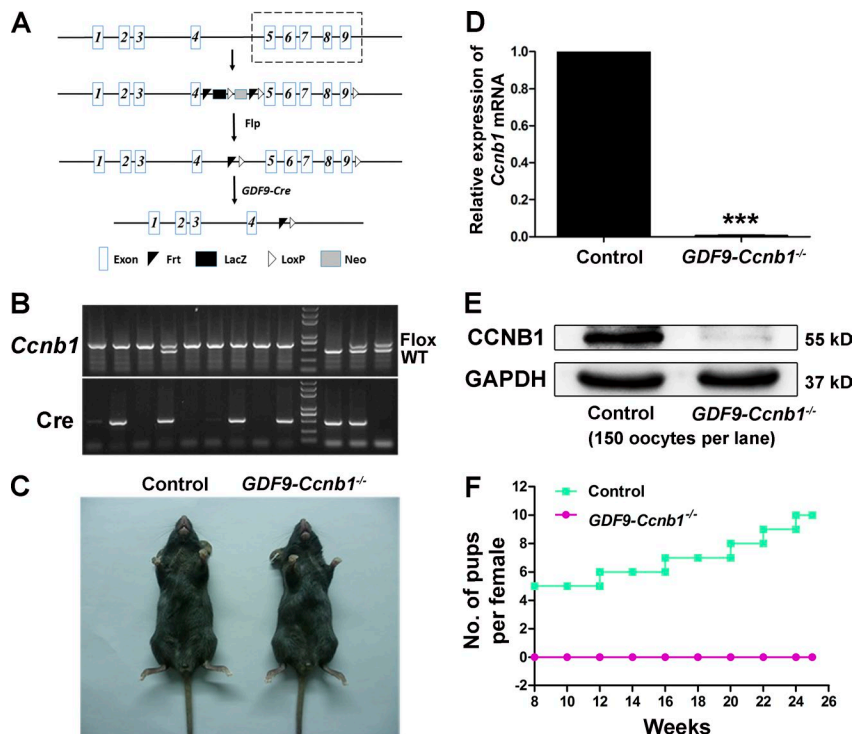*J. Li and J.-X. Tang contributed equally to this paper;   Correspondence to Yi-Xun Liu: liuyx@ioz.ac.cn.

Figure 1. **Infertility of the *GDF9-Ccnb1*−/− female mice. (A)** Construction of *Ccnb1^Flox/Flox^* and generation of *Ccnb1^Flox/Flox^;GDF9-Cre* mice. Exons 5–9 of *Ccnb1* were deleted by *GDF-9-Cre*–mediated recombination. **(B)** Genotyping PCR for the identification of the *GDF9-Ccnb1*−/− mice. The Flox band was 673 bp, and the WT band was 475 bp. **(C)** Morphology of the *GDF9-Ccnb1*−/− female mouse. The size of the *GDF9-Ccnb1*−/− female was comparable with the control female. **(D)** Real-time PCR showing the loss of *Ccnb1* mRNA in the *GDF9-Ccnb1*−/− mouse oocytes. 7-wk-old control and *GDF9-Ccnb1*−/− mice were used. *Gapdh* was used as the internal reference, and the mRNA expression of the control group was normalized to 1. ***, P < 0.0001. **(E)** Western blot demonstrating the absence of Cyclin B1 protein in the *GDF9-Ccnb1*−/− mouse oocytes. A total of 150 oocytes that underwent GVBD (after 2 h incubation in M2 medium at 37°C) were used in each lane, and the level of GAPDH was used as an internal control. The experiment was repeated three times. **(F)** Fertility curves of the *GDF9-Ccnb1*−/− female mice (*n* = 7; magenta line) and the control females (*n* = 7; green line).

and it was found that *Ccnb2*-null mice developed normally and were fertile, whereas *Ccnb1*-null mice died in utero, which suggests that Cyclin B1 is critical for embryonic development; nevertheless, Cyclin B2 is dispensable for embryonic development and fertility.

The well-established understanding about the critical function of Cyclin B1 in MPF activation and oocyte meiotic resumption are from in vitro studies (Kanatsu-Shinohara et al., 2000; Tay et al., 2000; Ledan et al., 2001; Peter et al., 2002; Huo et al., 2005; Holt et al., 2010, 2013; Adhikari and Liu, 2014), and the outcome of conventional *Ccnb1* knockout precludes the study of Cyclin B1 function in oocyte meiosis in vivo. In this study, we generated conditional knockout mice with oocyte-specific deletion of *Ccnb1* to investigate the requirement of Cyclin B1 for oocyte meiotic progression. We found that conditional knockout female mice were completely infertile. To our surprise, oocytes lacking Cyclin B1 showed elevated MPF activity and subsequent GVBD, which is unexpected. The *Ccnb1*-null oocytes completed the first meiosis as indicated by extruded the first polar body (PB1) and then entered interphase-like stage without metaphase of meiosis II (MII) arrest, which accounted for female infertility. The other important finding was that the activation of MPF in *Ccnb1*-null oocytes was due to up-regulation of Cyclin B2 expression, since knockdown of Cyclin B2 in *Ccnb1*-null oocytes arrested most oocytes at the GV stage. Furthermore, oocytes with double deletions of *Ccnb1* and *Ccnb2* were permanently arrested at the GV stage. Interestingly, exogenous Cyclin B2 could restore the MII arrest in the *Ccnb1*-null oocytes. Our findings have demonstrated that Cyclin B1 and Cyclin B2 may compensate each other in regulating MPF activity as well as the first meiotic resumption and second meiotic arrest in oocytes, which is important for understanding the regulatory mechanism of oocyte meiotic progression.

Results

Oocyte-specific deletion of Cyclin B1 results in female infertility

To delete Cyclin B1 (encoded by *Ccnb1*) in oocytes, we generated *Ccnb1^Flox/Flox^* mice. Subsequently, the *Ccnb1^Flox/Flox^* mice were crossed with the *GDF9-Cre* mice to obtain *Ccnb1^Flox/Flox^;GDF9-Cre* mice (referred to as *GDF9-Ccnb1*−/− mice; Fig. 1 A). We identified the genotype of *GDF9-Ccnb1*−/− mice by PCR (Fig. 1 B). The sizes of the *GDF9-Ccnb1*−/− female mice were comparable with those of controls (Fig. 1 C). Using real-time PCR and Western blot, we confirmed the absence of *Ccnb1* mRNA and protein in the *GDF9-Ccnb1*−/− mouse oocytes (Fig. 1, D and E; and Fig. S1 A). After mating for >6 mo, we found that the *GDF9-Ccnb1*−/− female mice were completely infertile (Fig. 1 F).

Oocytes undergo GVBD and PB1 extrusion (PBE) but fail to arrest at the MII in the absence of Cyclin B1

To explore the cause of infertility of *GDF9-Ccnb1*−/− female mice, we examined oocyte meiotic progression. We expected that oocytes would be arrested at the GV stage due to the absence of Cyclin B1 and thus failed activation of MPF. To our surprise, all ovulated oocytes from the *GDF9-Ccnb1*−/− female mice showed a PB1 and an interphase-like nucleus (Fig. 2, A and B). To characterize this nucleus state, we examined the level of DNA damage (Fig. 2 C) and the levels of trimethylated H3K9 (H3K9me3) and trimethylated H3K27 (H3K27me3; Fig. 2, D and E), which mediated the silence of condensed chromatin (Kimura, 2013). We thus examined early embryo development in the *GDF9-Ccnb1*−/− females. As shown in Fig. S1 B, no obvious embryo implantation sites were observed in *GDF9-Ccnb1*−/− mouse uteri at 6 d postcoitum (dpc). The number of embryos collected from the ampulla of oviducts in the *GDF9-Ccnb1*−/− females was comparative with the control at 1.5 dpc (Fig. S1 C), but no normal two-cell embryos were found (Fig. S2). After
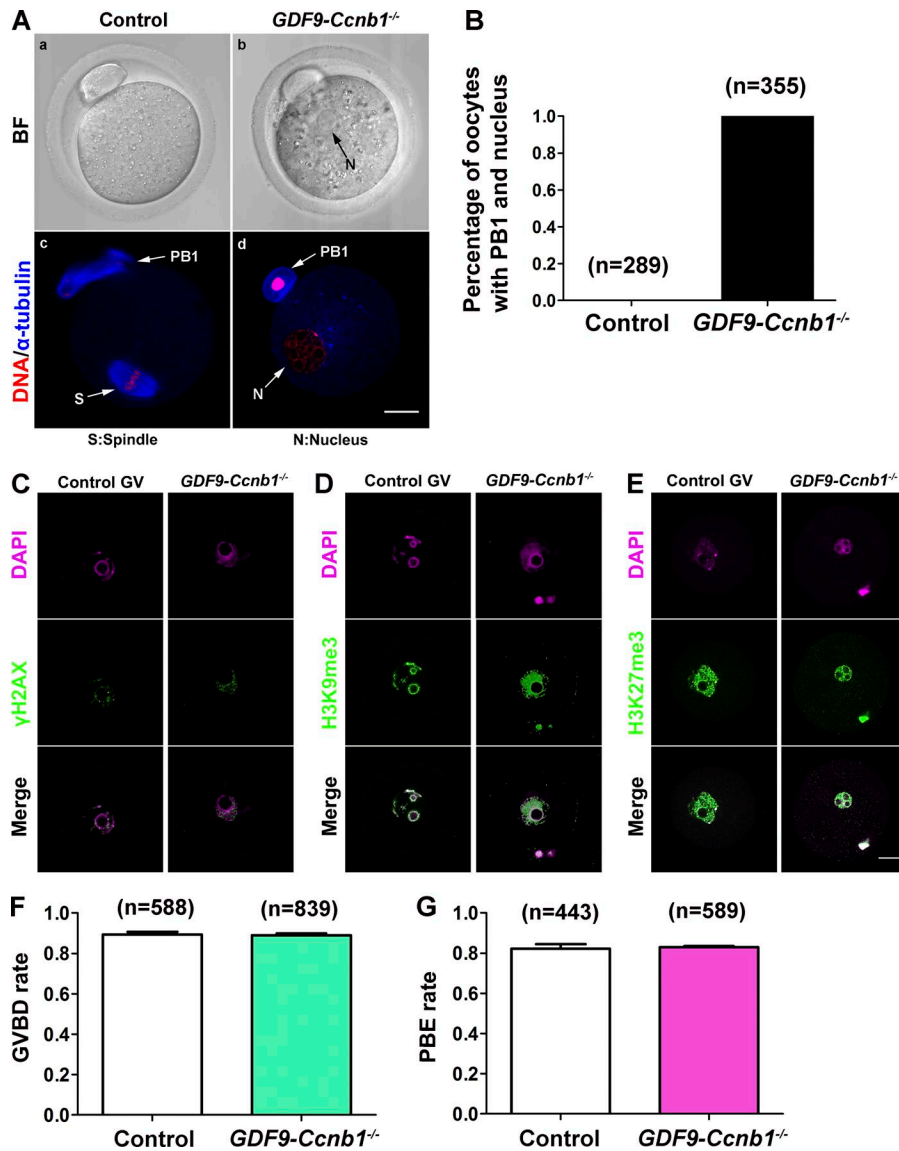
Figure 2. **The *GDF9-Ccnb1*^{-/-} oocytes resumed meiosis normally but failed to arrest at the MII after PBE. (A)** Entry into interphase after PBE in ovulated *GDF9-Ccnb1*^{-/-} oocytes. Control oocytes formed metaphase II spindles with condensed chromosomes after extrusion of PB1 (a and c). The *GDF9-Ccnb1*^{-/-} oocytes formed new nuclei with decondensed chromatin after extrusion of PB1 (b and d). BF, brightfield; S, spindle; N, nucleus. Bar, 20 µm. **(B)** The percentages of oocytes with nucleus formation after PBE. All the *GDF9-Ccnb1*^{-/-} oocytes formed nuclei after PBE, and no control oocytes formed nuclei. **(C)** Detection of DNA damage with phospho-histone H2A.X (γH2AX) staining in the *GDF9-Ccnb1*^{-/-} oocytes. **(D)** Characterization of chromatin compaction with H3K9me3 staining in the *GDF9-Ccnb1*^{-/-} oocytes. **(E)** Characterization of chromatin compaction with H3K27me3 staining in the *GDF9-Ccnb1*^{-/-} oocytes. In C–E, WT GV oocytes were used as the control, and 10 oocytes were used for staining in each group. Bars, 20 µm. **(F)** The GVBD rate of the *GDF9-Ccnb1*^{-/-} and control oocytes. The GVBD rate of *GDF9-Ccnb1*^{-/-} oocytes (89.39 ± 1.4%) was comparable with that of control oocytes (88.89 ± 1.0%). **(G)** The PBE rate of the *GDF9-Ccnb1*^{-/-} and control oocytes. The PBE rate of *GDF9-Ccnb1*^{-/-} oocytes (82.95 ± 0.7%) was also comparable with that of control oocytes (82.32 ± 2.2%). The GVBD and PBE rates were scored after 3-h and 14-h incubation periods, respectively. The numbers of oocytes used (*n*) are shown. Data are presented as mean ± SEM.

in vitro culture, these eggs did not further develop (Fig. S2). However, the ovary morphology and follicle development of the *GDF9-Ccnb1*^{-/-} ovary appeared to be normal (Fig. S3).

The unexpected oocyte phenotype prompted us to further examine meiosis I progression of the *GDF9-Ccnb1*^{-/-} oocytes. Strikingly, the GVBD and PBE rates in the *GDF9-Ccnb1*^{-/-} oocytes were comparable with those in the control group (Fig. 2, F and G). To further observe the meiotic progression of *GDF9-Ccnb1*^{-/-} oocytes, we conducted live-cell imaging of oocytes after microinjections with *H2B-mCherry* and *MAP7-EGFP* to label chromosomes and spindles, respectively (Fig. 3 A and Videos 1 and 2). This labeling enabled the monitoring of the dynamics of nuclear changes, spindle assembly, and chromosome segregation. The spindle morphology and chromosome alignment were similar to the controls (Fig. S4, A–D). During 18 h of observation, we recorded the schedule of oocyte meiosis. Compared with control oocytes, the *GDF9-Ccnb1*^{-/-} oocytes underwent GVBD and PBE at the normal time frame (Fig. S4, E and F), but chromosomes decondensed, spindles disassembled after PBE, and interphase-like nuclei formed after 4–6 h (Fig. S4 G). Microinjection

of moderate amount of *Ccnb1* mRNA restored the MII arrest in the *GDF9-Ccnb1*^{-/-} oocytes (Fig. S4 H), and inappropriate Cyclin B1 expression resulted in other two phenotypes: Cyclin B1 overexpression arrested the oocytes at metaphase of meiosis I (MI; Ledan et al., 2001), while insufficient Cyclin B1 had no effect (Fig. S4 H). These results show that, unexpectedly, resumption of the first meiosis of oocytes can occur in the absence of Cyclin B1, but expectedly, metaphase arrest of the second meiosis does need Cyclin B1 accumulation.

CDK1 is activated in meiosis I but inactivated in meiosis II in the absence of Cyclin B1

To determine why GVBD could occur in the *GDF9-Ccnb1*^{-/-} oocytes, we examined CDK1 activity. Because the phosphorylation and disassembly of nuclear lamina are downstream of CDK1 during GVBD (Heald and McKeon, 1990; Peter et al., 1990; Ward and Kirschner, 1990), we also verified phosphorylation of lamin A/C in the *GDF9-Ccnb1*^{-/-} oocytes at the time of GVBD. As shown in Fig. 3 B, the CDK1 activity in the *GDF9-Ccnb1*^{-/-} oocytes was comparable with that in the control oocytes, and the phosphor-
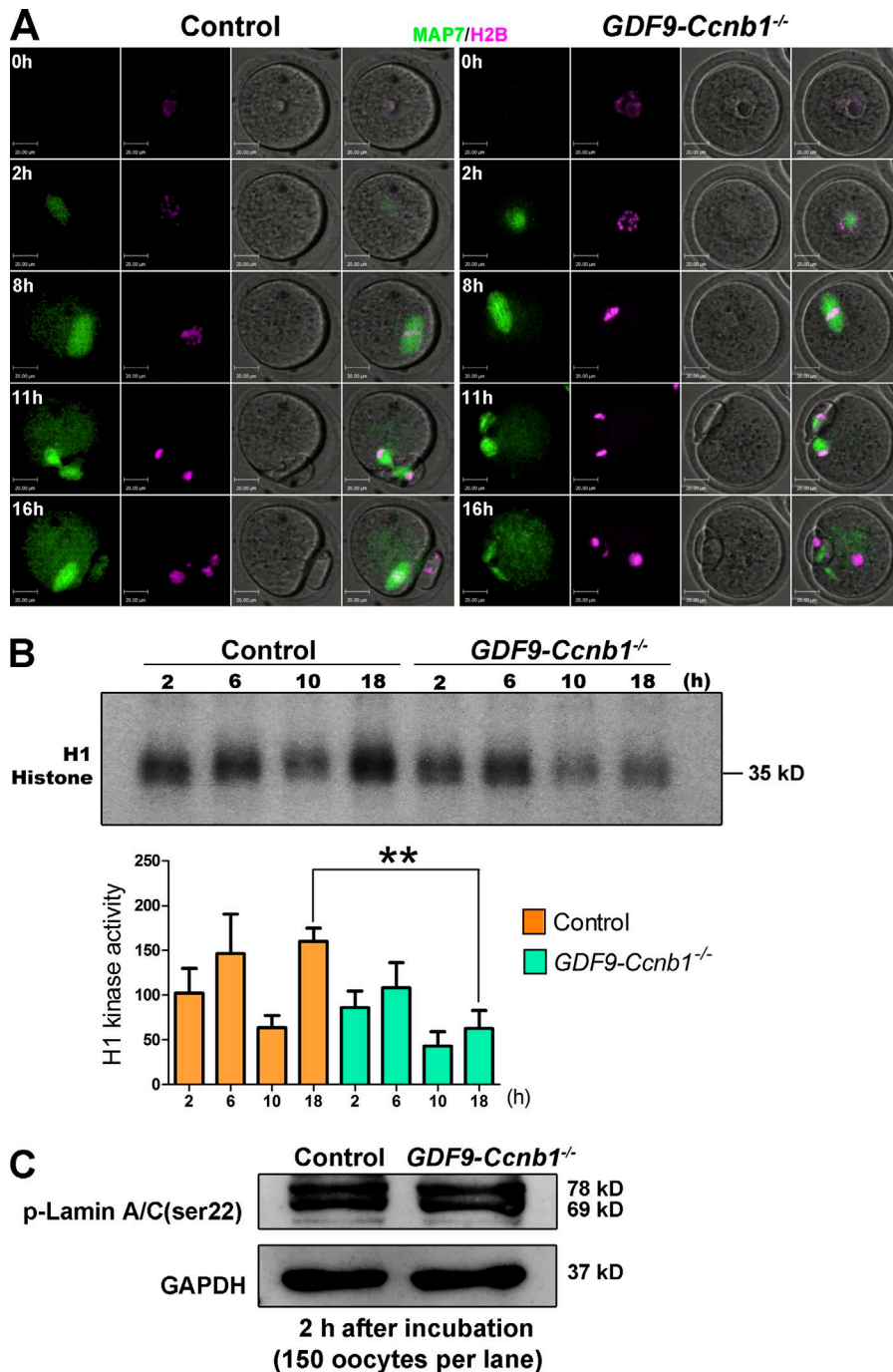
Figure 3. **CDK1 was active during GVBD but remained inactivated after PBE in the *GDF9-Ccnb1*−/− oocytes. (A)** Selected timeframes of a representative multichannel video of the *GDF9-Ccnb1*−/− (*n* = 93) and control oocytes (*n* = 68) progressing through meiosis. Chromosomes and spindle microtubules were visualized with H2B-mCherry and MAP7-EGFP, respectively. Bars, 20 µm. **(B)** Histone H1 kinase assay of the *GDF9-Ccnb1*−/− and control oocytes during meiosis. Oocytes were collected at certain time points (2, 6, 10, and 18 h), and 10 oocytes were used in each lane. CDK1 activity in the *GDF9-Ccnb1*−/− oocytes at 2, 6, or 10 h was comparable with that of control oocytes, but after PBE, the CDK1 activity in the *GDF9-Ccnb1*−/− oocytes remained at a low level. CDK1 activity in control oocytes was reactivated and peaked at 18 h. The mean kinase activity from three separate experiments is shown. Data are presented as mean ± SEM. **, P = 0.0079. **(C)** Phosphorylation detection of lamin A/C in the *GDF9-Ccnb1*−/− oocytes during GVBD. 150 oocytes were used in each lane.

ylation level of lamin A/C was also similar to that of the control (Fig. 3 C). However, unlike the control oocytes, the CDK1 activity in the *GDF9-Ccnb1*−/− oocytes did not exhibit a distinct increase after PBE but remained at a low level (Fig. 3 B). Thus, CDK1 could be activated in the first meiosis of oocytes, while it could not be reactivated in the second meiosis after PBE resulted in the failure of meiosis II in the absence of Cyclin B1.

Cyclin B2 is significantly up-regulated in *GDF9-Ccnb1*−/− oocytes

Given that CDK1 is activated in the *GDF9-Ccnb1*−/− oocytes in the absence of Cyclin B1, the major CDK1-activating cyclin, we

assumed the existence of a compensatory mechanism among cyclins. Therefore, we examined the expression of the B-type cyclin in mammals. By Western blotting, we found that Cyclin B2 was significantly up-regulated in the *GDF9-Ccnb1*−/− oocytes during GVBD (Fig. 4 A). However, after PBE, Cyclin B2 remained at an extremely low level (Fig. 4 A). This result was in accordance with the CDK1 activity assay in the *GDF9-Ccnb1*−/− oocytes. Additionally, CDK1 plays its role of phosphorylation in the nucleus to promote GVBD (Li et al., 1997; Yang et al., 1998). Thus, Cyclin B2 was likely imported into the nucleus before GVBD in the *GDF9-Ccnb1*−/− oocytes to activate CDK1. To confirm the nuclear import of Cyclin B2, we constructed a Cyclin B2–Venus probe to trace
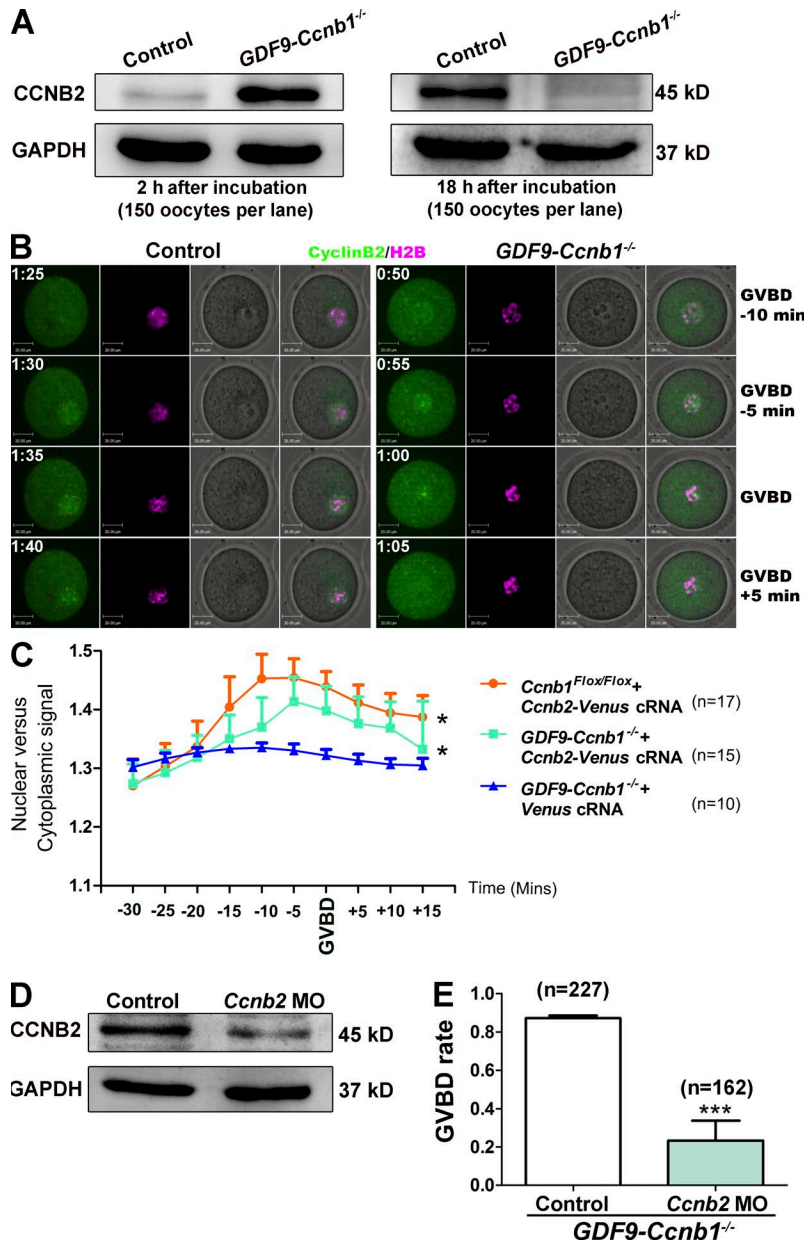
A

B

C

D

E

Figure 4. **Up-regulation of Cyclin B2 during GVBD in the *GDF9-Ccnb1^−/−* oocytes.** **(A)** Western blot of Cyclin B2 in the *GDF9-Ccnb1^−/−* oocytes. Cyclin B2 displayed an apparent increase in the *GDF9-Ccnb1^−/−* oocytes during GVBD, but it showed weak expression after PBE. 150 oocytes were used in each lane. **(B)** Nuclear import of Cyclin B2 in mouse oocytes during GVBD. GV-stage oocytes were microinjected with *Ccnb2-Venus* and *H2B-mCherry* cRNAs, and after 2 h incubation in IBMX, the oocytes were released from IBMX to undergo GVBD. For both the *GDF9-Ccnb1^−/−* oocytes (n = 17) and control oocytes (n = 15), Cyclin B2–Venus fluorescence was concentrated in the nucleus at 10–20 min before GVBD. The time is shown (h:min). Bars, 20 μm. **(C)** Ratio of nuclear versus cytoplasmic Cyclin B2–Venus fluorescence in oocytes. The nuclear and cytoplasmic Cyclin B2–Venus fluorescence intensities were measured every 5 min from 30 min before GVBD to 15 min after GVBD in the control and *GDF9-Ccnb1^−/−* oocytes. Then, the ratio of nuclear versus cytoplasmic signal was calculated. The numbers of oocytes used (n) are shown. *, $P < 0.05$. **(D)** Western blot of Cyclin B2 in the Cyclin B2–knockdown oocytes. Following microinjection of *Ccnb2* MO, Cyclin B2 was decreased markedly in oocytes. After microinjection, the oocytes were incubated in IBMX for 24 h. 150 oocytes were used in each lane. **(E)** Cyclin B2 interference in the *GDF9-Ccnb1^−/−* oocytes induced severe GV arrest. GVBD rate in the *GDF9-Ccnb1^−/−* oocytes after Cyclin B2 interference. After microinjection with *Ccnb2* MOs, the microinjected *GDF9-Ccnb1^−/−* oocytes were released into M2 medium to undergo GVBD following 24 h incubation in IBMX. GVBD was severely suppressed after Cyclin B2 interference (23.35% ± 4.2%) compared with the noninjected *GDF9-Ccnb1^−/−* oocytes (87.18% ± 0.6%). GVBD rates were scored at 3 h incubation in M2 medium. Data are presented as mean ± SEM. ***, $P < 0.0001$.

the localization of Cyclin B2 in oocytes. Using real-time monitoring, we observed that Cyclin B2–Venus emerged in the nucleus at 10–20 min before GVBD (Fig. 4, B and C; and Videos 3 and 4). This phenomenon was captured in both the control and *GDF9-Ccnb1^−/−* oocytes. Therefore, Cyclin B2 may compensate Cyclin B1 function in CDK1 activation and subsequent GVBD stimulation.

Cyclin B2 knockdown suppresses GVBD in *GDF9-Ccnb1^−/−* oocytes

To further verify that Cyclin B2 compensated the loss of Cyclin B1 in the *GDF9-Ccnb1^−/−* oocytes, we performed RNAi by microinjection of morpholino oligonucleotides (MOs) that targeted *Ccnb2* mRNA to knockdown Cyclin B2 in the *GDF9-Ccnb1^−/−* oocytes. First, we tested the effectiveness of MOs using WT oocytes. As shown in Fig. 4 D, Cyclin B2 was down-regulated in the MO-injected oocytes. After Cyclin B2 knockdown in the *GDF9-Ccnb1^−/−* oocytes, the GVBD rate sharply decreased (Fig. 4 E), suggesting

that Cyclin B2 promoted the resumption of meiosis in the absence of Cyclin B1.

Ccnb1 and *Ccnb2* double knockout permanently arrests the oocytes at the GV stage

To ascertain the compensatory function of Cyclin B2 in vivo, we successfully established *Ccnb2*-knockout mice with a CRISPR-Cas9 system (Fig. 5 A), and the mice were identified at DNA level (Fig. 5 B), mRNA level (Fig. 5 C), and protein level (Fig. 5 D). The *Ccnb2^−/−* female mice were fertile, as reported previously (Brandeis et al., 1998), and then they were crossed with *GDF9-Ccnb1^−/−* male mice to generate *GDF9-Ccnb1^−/−;Ccnb2^−/−* female mice (Fig. 5, E and F) whose oocytes lacked both Cyclin B1 and Cyclin B2. After superovulation, oocytes were collected from oviducts 16 h after human chorionic gonadotropin (HCG) injection. In the *GDF9-Ccnb1^−/−;Ccnb2^−/+* females, most oocytes were arrested at second meiotic interphase, like *GDF9-Ccnb1^−/−*

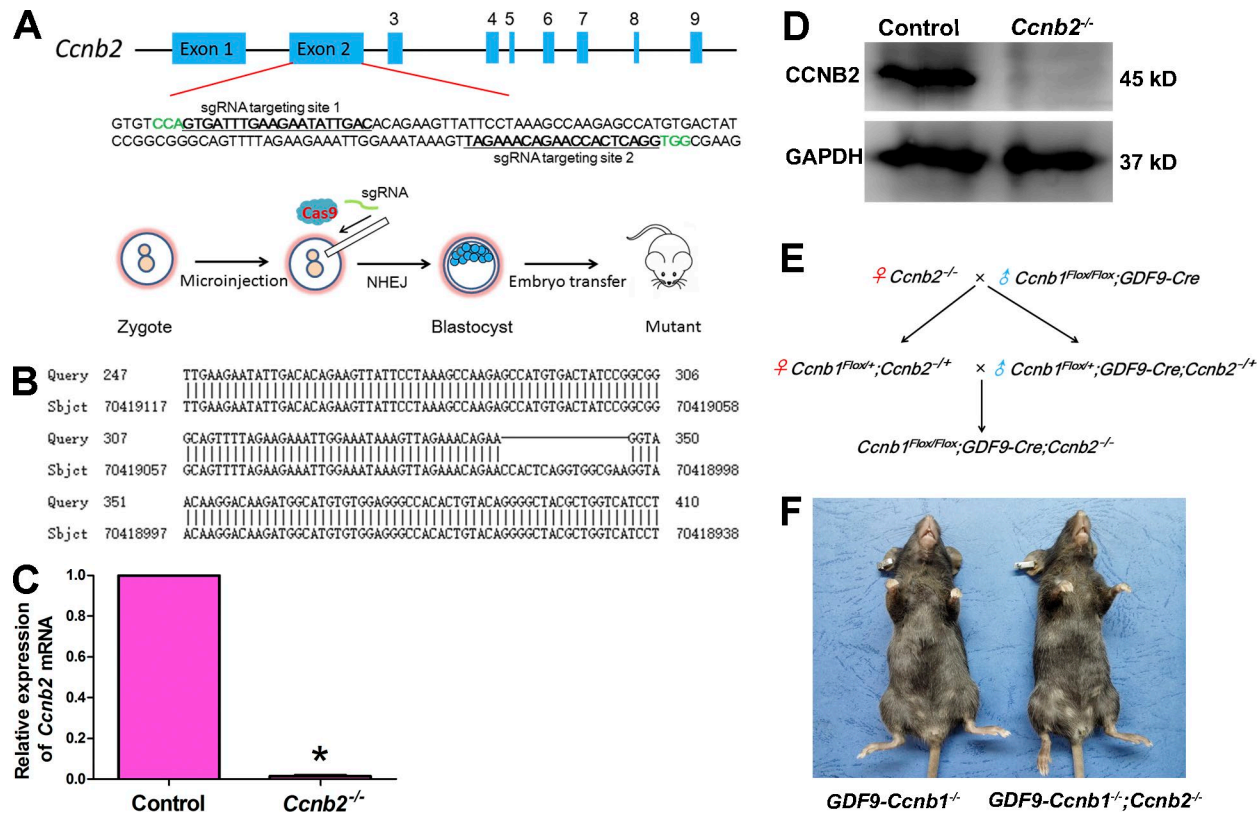**Figure 5. Construction of *Ccnb2*-knockout mice with the CRISPR-Cas9 system and generation of the *GDF9-Ccnb1⁻/⁻;Ccnb2⁻/⁻* mice. (A)** Schematic diagram of *Ccnb2* knockout in mice. The sgRNAs were designed to target the exon 2 of *Ccnb2* gene. NHEJ, nonhomologous end joining. **(B)** Sequence alignment for exon 2 in the *Ccnb2⁻/⁻* mice. 16 bp were lost in exon 2 of *Ccnb2⁻/⁻* mice, resulting in the reading frame shift mutation. **(C)** Quantitative analysis of the expression of *Ccnb2* mRNA in the *Ccnb2⁻/⁻* mouse ovary. *Gapdh* was used as the internal reference, and the mRNA expression of the control group was normalized to 1. Data are presented as mean ± SEM. *, P < 0.05. **(D)** Western blot for Cyclin B2 protein expression in the *Ccnb2⁻/⁻* mouse ovary. **(E and F)** Optimized mating strategy to produce the *GDF9-Ccnb1⁻/⁻; Ccnb2⁻/⁻* female mice and morphology of the mouse.

oocytes, and few oocytes remained at the GV stage (Fig. 6 A). In contrast, in the *GDF9-Ccnb1⁻/⁻;Ccnb2⁻/⁻* females, all oocytes were arrested at the GV stage (Fig. 6 A). When oocytes were collected from ovaries to culture in vitro, GVBD occurred in the majority of WT oocytes within 1.5 h, while GVBD of *GDF9-Ccnb1⁻/⁻;Ccnb2⁻/+* oocytes was delayed, and GVBD of *GDF9-Ccnb1⁻/⁻;Ccnb2⁻/⁻* oocytes did not occur after extended culture (Fig. 6 B), as is the case in vivo. The *GDF9-Ccnb1⁻/⁻;Ccnb2⁻/⁻* oocytes remained at the GV stage even after extended culture for 2 d (Fig. S5 A). Hence, it demonstrated that Cyclin B2 compensated for the function of Cyclin B1 to regulate oocyte meiotic resumption.

Cyclin B2 expression triggers GVBD of *GDF9-Ccnb1⁻/⁻;Ccnb2⁻/⁻* oocytes

To further solidify the observation that Cyclin B2 can take on the role of Cyclin B1 in driving meiotic resumption, we then injected *Ccnb2* mRNA into the *GDF9-Ccnb1⁻/⁻;Ccnb2⁻/⁻* oocytes to observe whether this could trigger the GVBD. To our expectation, most of the *Ccnb2*-injected oocytes underwent GVBD even in the presence of inhibitor 3-isobutyl-1-methylxanthine (IBMX; Fig. 6 C), and the rest of the *Ccnb2*-injected oocytes underwent GVBD after release from IBMX. In contrast, the Venus-injected oocytes remained at the GV stage (Fig. 6 C). This result strongly suggests

that Cyclin B2 can substitute for Cyclin B1 in promoting the resumption of meiosis in mouse oocytes.

Cyclin B2 expression restores the MII arrest in the *GDF9-Ccnb1⁻/⁻* oocytes

The *GDF9-Ccnb1⁻/⁻* oocytes could not arrest at the MII stage because of the inactivation of MPF, and Cyclin B2 protein was absent at this time (Fig. 4 A). To clarify whether exogenous Cyclin B2 expression could drive the interphase-like oocytes back to MII stage in the *GDF9-Ccnb1⁻/⁻* oocytes, we introduced *Ccnb2* mRNA into the GV-intact *GDF9-Ccnb1⁻/⁻* oocytes and released the oocytes for maturation after 3 h incubation in IBMX. We found that many *GDF9-Ccnb1⁻/⁻* oocytes were arrested at the MII stage after forced expression of Cyclin B2 (Fig. 6 D), while some oocytes seemed to be arrested at the MI stage (Fig. 6 D), which was similar to the phenotype of Cyclin B1 overexpression (Fig. S4 H). This result indicates that Cyclin B2 can take on the role of Cyclin B1 to activate MPF for maintaining MII arrest in oocytes.

Cyclin B2 deletion delays the resumption of meiosis in mouse oocytes

Besides, we also found that the *Ccnb2⁻/⁻* oocytes underwent GVBD slowly (Fig. S5 B). Introduction of *Ccnb1* mRNA rescued the GVBD to some extent, but the GVBD rate could not reach the
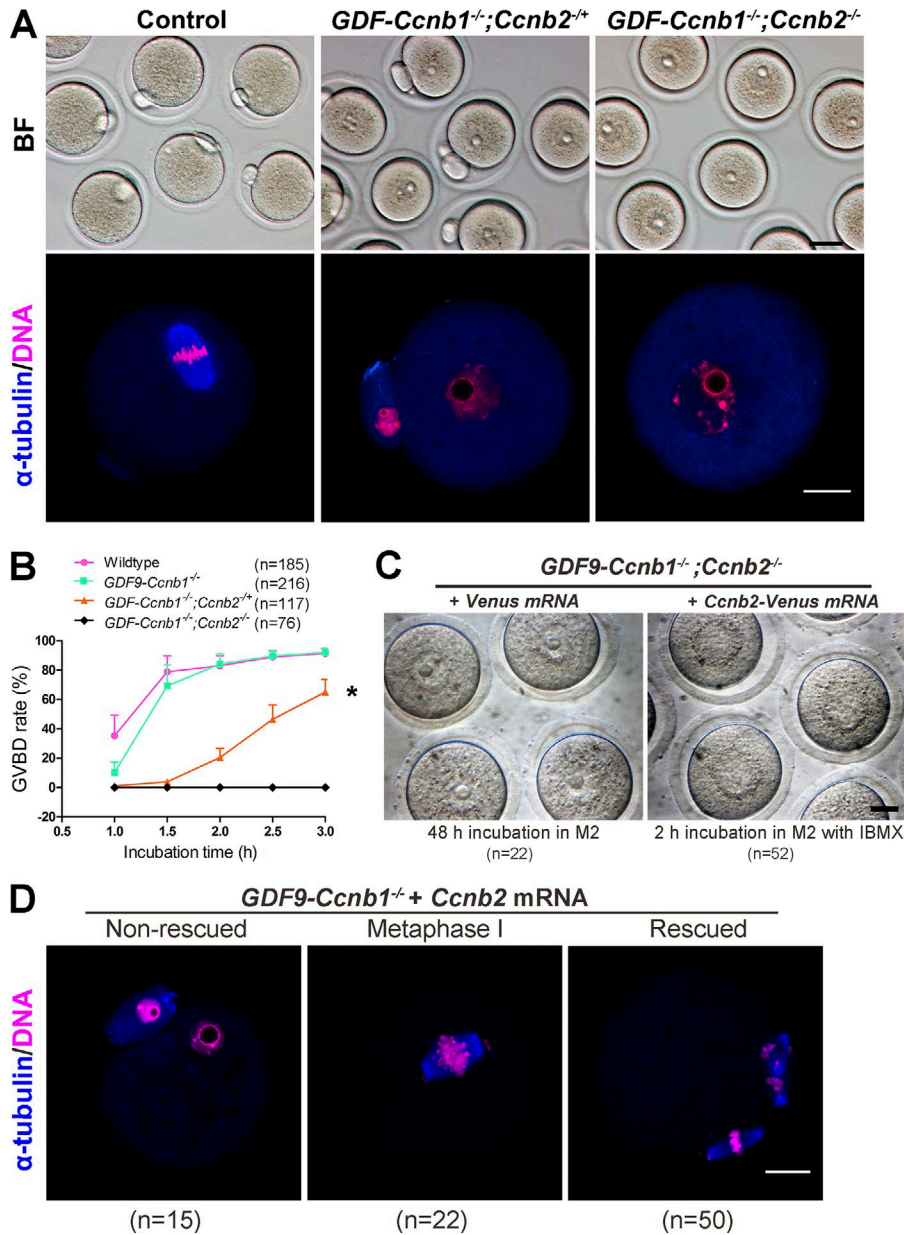
Figure 6. **Oocytes lacking both Cyclin B1 and Cyclin B2 were permanently arrested at the GV stage. (A)** Morphological observation and immunofluorescent staining for the ovulated oocytes in the *GDF9-Ccnb1⁻/⁻;Ccnb2⁻/⁻* female mice. Oocytes were collected from the oviducts 16 h after HCG injection. Control (*n* = 52), *GDF9-Ccnb1⁻/⁻;Ccnb2⁻/⁺* (*n* = 28), and *GDF9-Ccnb1⁻/⁻;Ccnb2⁻/⁻* (*n* = 44) were used. Bars: 40 μm (A, brightfield [BF]); 20 μm (A, immunofluorescence). **(B)** GVBD was blocked completely in the *GDF9-Ccnb1⁻/⁻;Ccnb2⁻/⁻* mouse oocytes after culture in vitro. The numbers of oocytes used (*n*) are shown. Data are presented as mean ± SEM. *, P < 0.05. **(C)** Rescue of GVBD by Cyclin B2 in the *GDF9-Ccnb1⁻/⁻;Ccnb2⁻/⁻* oocytes. Microinjection of *Ccnb2* mRNA into the *GDF9-Ccnb1⁻/⁻;Ccnb2⁻/⁻* oocytes overcame the GV arrest, and most oocytes underwent GVBD in the presence of IBMX. Bar, 20 μm. **(D)** Restoration of MII arrest by exogenous Cyclin B2 in the *GDF9-Ccnb1⁻/⁻* oocytes. *Ccnb2* mRNA was introduced into the GV-intact *GDF9-Ccnb1⁻/⁻* oocytes, which were released into IBMX-free M2 medium after 2 h incubation in the M2 containing IBMX. At 16 h after GVBD, α-tubulin and DNA staining were performed, and the oocytes also showed three phenotypes similar to the results by *Ccnb1* introduction (Fig. S4 H). Bar, 20 μm. The numbers of oocytes used (*n*) are shown in C and D.

Discussion

MPF, a Cyclin B–CDK1 complex, is responsible for the initiation of G2/M transition and M-phase entry in meiotic oocytes (Polánski et al., 2012). Cyclin B1 is regarded as the major partner regulating CDK activity and key events of oocyte meiotic maturation. It is well known that synthesis and degradation of Cyclin B1 regulates the timing of meiotic progression, especially GV arrest/GVBD, metaphase–anaphase transition of the first meiosis, and metaphase arrest/exit of the second meiosis. CDK1-null oocytes are permanently arrested at the GV stage (Adhikari et al., 2012), indicating that CDK1 activity is essential for stimulating the resumption of first meiosis in mouse oocytes. Normally, the activity of CDK1 depends on the accumulation of Cyclin B1. Loss of Cyclin B1 would be expected to inhibit the occurrence of GVBD. Surprisingly, *GDF9-Ccnb1⁻/⁻* oocytes underwent GVBD normally (Fig. 3 A and Videos 1 and 2). Both GVBD and PBE occurred at a comparable time frame and rate compared with control oocytes (Fig. 2, F and G). To address why GVBD occurred in the absence of Cyclin B1, we examined CDK1 activity during GVBD in *Ccnb1*-null oocytes, and surprisingly, we found that CDK1 was activated, and its downstream lamin A/C was phosphorylated in the absence of Cyclin B1, which is in contrast with our previous understandings about the regulatory mechanism

normal level (Fig. S5 B). Given that the *GDF9-Ccnb1⁻/⁻* oocytes underwent GVBD normally, this finding suggests that Cyclin B2 may play an unexpected important role that could not be completely compensated in a short period by Cyclin B1 during the resumption of meiosis in mouse oocytes. The *Ccnb2⁻/⁻* oocytes that underwent GVBD could extrude polar bodies after extended in vitro culture (not depicted), suggesting that Cyclin B1 alone was capable of promoting the meiosis I/meiosis II transition, which accounted for the fertility of the *Ccnb2⁻/⁻* female mice.

of MPF activation and meiotic resumption in oocytes (Holt et al., 2010; Adhikari and Liu, 2014).

The different meiotic oocyte phenotypes after oocyte-specific deletions of Cyclin B1 and CDK1 prompted us to clarify the reasons. Although traditional *Ccnb2* knockout mice were viable, compensation of Cyclin B1 function by Cyclin B2 in contributing to CDK1 activity and meiotic resumption was possible in *Ccnb1*-null oocytes because the translation of Cyclins B1 and B2 is differentially regulated (Han et al., 2017). Indeed, we found that expression of Cyclin B2 was elevated in *GDF9-Ccnb1*$^{-/-}$ oocytes, and knockdown of Cyclin B2 arrested most of the *Ccnb1*-null oocytes at the GV stage. More convincingly, double knockout of *Ccnb1* and *Ccnb2* permanently arrested oocytes at the GV stage. Our further findings showed that expression of Cyclin B2 could trigger the GVBD of *GDF9-Ccnb1*$^{-/-}$;*Ccnb2*$^{-/-}$ oocytes and that the GVBD of *Ccnb2*-null oocytes was delayed, although *Ccnb2*-null females are fertile, suggesting an important role of Cyclin B2 in regulating meiotic resumption. Our solid evidence suggests that Cyclin B2 compensates Cyclin B1 function in MPF activation and subsequent meiotic resumption as well as vice versa. These findings will help to further understand the regulation of oocyte meiotic resumption.

In the *GDF9-Ccnb1*$^{-/-}$ oocytes, even though Cyclin B1 was redundant for the resumption of the first meiosis, CDK1 failed to reactivate after PBE, and oocytes entered interphase-like arrest, suggesting that Cyclin B1 was essential for metaphase arrest of the second meiotic division. The dynamic changes of chromosomes and spindles in the *GDF9-Ccnb1*$^{-/-}$ oocytes were normal during meiosis I. However, after PBE, chromosome decondensation and spindle disassembly occurred, followed by interphase-like nucleus reformation. Similarly, oocytes with deletion of Great-wall kinase entered the S phase after PBE (Adhikari et al., 2014). The factors enabling Cyclin B2 compensation for Cyclin B1 function in the resumption of first meiosis and subsequent M-phase entry but not in chromosome condensation and metaphase arrest of meiosis II remains unclear. In *Xenopus laevis* oocytes, new synthesis of B-type cyclins is required for the transition from meiosis I to meiosis II, during which Cyclins B1 and B4 play major roles, while in some cases, Cyclins B2 and B5 may compensate their functions (Hochegger et al., 2001). Given that both Cyclin B1 and Cyclin B2 are substrates of anaphase-promoting complex/cyclosome (APC/C; Thornton and Toczyski, 2003; Murray, 2004; Reis et al., 2006; Dimova et al., 2012; Touati et al., 2012; Gui and Homer, 2013), one possibility could be that the accumulation of Cyclin B2 after PBE was too slow to achieve the threshold for reactivating CDK1 in the *GDF9-Ccnb1*$^{-/-}$ oocytes due to excessive Cyclin B2 degradation by APC/C activity in the absence of Cyclin B1, and introduction of *Ccnb2* mRNA into the *GDF9-Ccnb1*$^{-/-}$ oocytes could restore the MII arrest (Fig. 6 D), implying that Cyclin B2 was destroyed completely by APC/C in the *GDF9-Ccnb1*$^{-/-}$ oocytes. In WT mouse oocytes, Cyclin B1 is not completely destroyed at the meiosis I/meiosis II transition. Detectable levels of Cyclin B1 remain upon exit from meiosis I (Huo et al., 2005; Polánski et al., 2012), indicating that residual Cyclin B1 may facilitate the rapid reactivation of CDK1 during meiosis II. When Cyclin B1 was completely deleted in the *GDF9-Ccnb1*$^{-/-}$ mouse oocytes, CDK1 activity could not be timely reactivated. However, this may be due to the difference between meiosis and mitosis: the second meiotic

division is analogous to mitosis, wherein Cyclin B1 is essential for metaphase initiation (Fung et al., 2007; Strauss et al., 2018). In this sense, it is reasonable to understand why the *GDF9-Ccnb1*$^{-/-}$ oocytes could not arrest at the MII.

In conclusion, our study shows that Cyclin B2 could substitute for Cyclin B1 to drive the activation of MPF and resumption of the first meiosis and that Cyclin B2 could compensate Cyclin B1's function in metaphase arrest of the second meiosis (Fig. 6 D). Our findings reveal an unknown compensatory mechanism between Cyclin B1 and Cyclin B2, providing new knowledge of the interchangeable functions of Cyclin B members during oocyte meiotic resumption.

Materials and methods

Mice

An embryonic stem cell line (clone EPD0357_2_A11) from The European Conditional Mouse Mutagenesis Program with the *Ccnb1* gene was used for microinjection to generate a *Ccnb1*$^{Flox/Flox}$ mouse model (on a C57BL/6 background) as previously reported (Tang et al., 2017). The PCR product from the *Ccnb1*$^{Flox/Flox}$ mice was 673 bp, whereas the PCR product from WT mice was 475 bp. The *Ccnb1*$^{Flox/Flox}$;*GDF9-Cre* (referred to as *GDF9-Ccnb1*$^{-/-}$) mice were generated by crossing *Ccnb1*$^{Flox/Flox}$ mice with transgenic mice carrying *GDF-9* promoter–mediated Cre recombinase (Lan et al., 2004).

Ccnb2-knockout mice were generated using a CRISPR-Cas9 system. The designed single guide RNA (sgRNA)-1/2 targeted exon 2 of *Ccnb2*. The sgRNA-1/2 and Cas9 nickase mRNAs were transcribed in vitro and coinjected into mouse zygotes. Injected zygotes were cultured in M16 medium (Sigma-Aldrich) at 37°C and 5% CO_2 for 2 or 3 d and then transplanted into the oviducts of pseudopregnant mice. The exon 2 of pups was amplified by PCR using the following primers: forward, 5′-GAATTGAACCCA GTCCACAG-3′, and reverse, 5′-TCTGCACTGGTTTCACAGAG-3′. Deletion of the *Ccnb2* gene was validated by DNA sequencing. All experimental protocols and animal handling procedures were conducted in accordance with the guidelines and procedures approved by the Institutional Animal Care Committee of the Institute of Zoology at the University of Chinese Academy of Sciences.

Fertility testing

For fertility testing, 6- to 8-wk-old *Ccnb1*$^{Flox/Flox}$ (control; *n* = 7) and *Ccnb1*$^{Flox/Flox}$;*GDF9-Cre* females (*n* = 7) were separately mated with WT C57BL/6 males for >6 mo. Litter sizes were assessed.

Histological analysis

2-wk, 4-wk, and 7-wk-old *Ccnb1*$^{Flox/Flox}$ and *Ccnb1*$^{Flox/Flox}$;*GDF9-Cre* female mice from the same litter were used. After euthanization via cervical dislocation, ovaries were isolated, individually fixed in 4% PFA in PBS for up to 24 h, and then stored in 70% ethanol and embedded in paraffin. Tissue sections (5 µm thick) were cut and mounted on glass slides. Sections were deparaffinized, rehydrated, and then stained with H&E staining.

Oocyte collection and culture

6- to 8-wk-old female mice were used. Mice were injected intraperitoneally with 10 U pregnant mare serum gonadotrophin.

After 44–48 h, GV-stage oocytes were collected from the ovary, and surrounding cumulus cells were removed mechanically. For in vitro maturation, denuded oocytes were cultured in M2 medium (M7167; Sigma-Aldrich) for microinjection. Oocytes were incubated in M2 medium containing 50 µm IBMX at 37°C.

Morpholino synthesis, cRNA preparation, and microinjection

MOs (5′-CCGCCCTGGCAAGTGCGGACGA-3′) for depleting murine Cyclin B2 were synthesized by Gene Tools according to mCCNB2 (NM_007630; encoding *Ccnb2*; Gui and Homer, 2013). *H2B-mCherry* and *MAP7-EGFP* cRNAs were made from a pMDL-H2B-mCherry vector and a pGEM-MAP7-EGFP vector through in vitro transcription (T3 or T7 mMessage mMachine [Ambion] according to the manufacturer's instructions), respectively. Mouse *Ccnb2* gene (NM_007630.2) was cloned into a pcDNA3.1-Venus vector, and its cRNA was prepared using T7 mMessage mMachine (Ambion). Mouse *Ccnb1* gene (NM_172301.3) was cloned into a pCS2+ vector, and its cRNA was prepared using SP6 mMessage mMachine (Ambion). All cRNAs were purified with RNeasy Mini kits (QIAGEN), dissolved in nuclease-free water, and stored at –80°C. A concentration of 500 ng/µl was used for microinjection. Microinjection was performed with a Nikon operating system.

Time-lapse confocal live imaging

Live imaging was performed using a PerkinElmer Ultra VIEW-VoX confocal imaging system equipped with an a CO_2 incubator chamber (5% CO_2 at 37°C) in M2 medium covered by mineral oil. The digital time-lapse images (26 z slices with 2-µm spacing) were acquired using a 20 × 0.75 objective lens, and Volocity 6.0 software was used for image acquisition. Injected oocytes were incubated in M2 medium supplemented with 50 µm IBMX for 3 h at 37°C and 5% CO_2. Then, the oocytes were released into M2 medium and prepared for time-lapse imaging. To image oocyte maturation with H2B-mCherry and MAP7-EGFP, images were taken every 20 min for 18 h. To image oocyte GVBD with Cyclin B2–Venus and H2B-mCherry, images were taken every 5 min for 4 h. Spindle length, spindle width, equatorial plate width, and fluorescence intensity were measured using Volocity 6.0 software.

Histone H1 kinase assay

Histone H1 kinase assays were performed according to a previously described protocol (Kubiak, 2013). 10 oocytes in a 24-µl reaction volume were prepared for each sample. Reactions were performed in a buffer containing 80 mM β-glycerophosphate, 15 mM MgCl$_2$, 20 mM EGTA, pH 7.3, 1 mM DTT, 1 mM AEBSF, 1 mg/ml leupeptin, 1 mg/ml pepstatin, 1 mg/ml aprotinin, 3.3 mg/ml histone H1 (Roche), 1 mM ATP, and 0.25 mCi/µl (^{32}P)-ATP (PerkinElmer), and samples were incubated at 37°C for 50 min. Samples were heated for 5 min at 90°C in SDS sample buffer and separated on a 10% SDS-PAGE. Radioactive signals were detected by exposing the gels to x-ray film in a dark room.

Confocal imaging and immunofluorescence analysis

The images of brightfield oocytes were acquired using an LSM 780 microscope (ZEISS) equipped with a Plan Apochromat 40 × 1.20 water-immersion objective lens (ZEISS) at RT, and Zen software (2010; ZEISS) was used for image acquisition. For spindle and DNA staining, ovulated oocytes collected from the oviduct 16 h after HCG injection were fixed in 4% PFA in PBS buffer for at least 30 min at RT before permeabilization for 20 min with 0.5% Triton X-100 at RT. The samples were then blocked in PBS containing 1% BSA for 1 h at RT. The oocytes were incubated with an anti–α-tubulin–FITC antibody (Thermo Fisher Scientific) overnight at 4°C. The following morning, oocytes were washed three times in wash buffer (PBS containing 0.1% Tween-20 and 0.01% Triton X-100) and then costained with DAPI (1 µg/ml in PBS; Sigma-Aldrich) for 15 min. Finally, the oocytes were mounted on glass slides and imaged with a confocal laser-scanning microscope (TCS SP8; Leica Microsystems) equipped with a high-contrast Plan Apochromat 40 × 1.10 water-immersion objective lens (Leica Microsystems) at RT, and Application Suite X software (2.0.0.14332; Leica Microsystems) was used for image acquisition. For p-H2A.X, H3K9me3, and H3K27me3 immunofluorescence staining, the following primary antibodies were used: anti–phospho-histone H2A.X antibody (rabbit; 9718; Cell Signaling Technology), anti-H3K9me3 antibody (rabbit; ab8898; Abcam), and anti-H3K27me3 antibody (rabbit; 2919706; EMD Millipore). Oocytes were incubated with primary antibodies at 4°C overnight and then incubated with donkey anti-rabbit secondary antibody (711-545-152; Jackson ImmunoResearch Laboratories, Inc.) for 1 h at RT, and DAPI was used to visualize the DNA.

RT-PCR and quantitative RT-PCR

To extract RNA from oocytes, 20 GV-intact denuded oocytes were lysed in 10 µl lysis buffer (5 mM DTT, 20 U/ml RNase inhibitor, and 1% NP-40) on ice for 30 min. RNA was extracted using an RNeasy Micro Kit (74004; QIAGEN) according to the manufacturer's protocols. To extract RNA from the ovary, the total RNA was extracted using TRIzol. The RNA samples were reverse-transcribed with Moloney murine leukemia virus reverse transcription (TIANGEN) and real-time quantitative PCR with GoTaq qPCR Master Mix (A6001/2; Promega) according to the manufacturer's protocols. Primers for quantitative RT-PCR were as follows: *Gapdh* forward, 5′-GGAGAAACCTGCCAAGTATG-3′, and reverse, 5′-GGAGAAACCTGCCAAGTAT G-3′; *Ccnb1* forward, 5′-GAGCTATCCTCATTGACTGG-3′, and reverse, 5′-CATCTTCTTGGG CACACAAC-3′; and *Ccnb2* forward, 5′-GCCAAGAGCCATGTGACT ATC-3′, and reverse, 5′-CAGAGCTGGTACTTTGGTGTTC-3′. Relative expression levels were calculated by the $2^{\Delta\Delta Ct}$ (threshold cycle) method: $\Delta\Delta Ct = \Delta Ct$ – maximal ΔCt, $\Delta Ct = Ct$ (*Ccnb1*) – Ct (*Gapdh*), and finally, the expression of control group was normalized to 1 by self-division.

For genotyping, mouse tail fractions were excised and lysed as templates. PCR was performed using a Master Mix (TSI NGKE) according to the manufacturer's protocols. Primers for the genotyping PCR were as follows: *Ccnb1* forward, 5′- CAAGCA CTTTACCACCGAACTAT-3′, and reverse, 5′-GTCAGAAGACAG CTACTGTGTAC-3′.

Western blotting

For protein extraction, 150 denuded oocytes were collected and added to 10 µl protein extraction buffer (100 mM NaCl, 20 mM Tris-HCl, pH 7.5, 0.5% Triton X-100, and 0.5% NP-40) containing the protease inhibitors PMSF (1 mM) and leupeptin-pepstatin

(1 µg/ml; Worrad et al., 1994). Extracts were briefly vortexed, centrifuged, and frozen at –80°C overnight. The samples were added to 5× SDS loading buffer and boiled for 5 min before being subjected to SDS-PAGE. Proteins were resolved on a prepared 5% stacking gel for 30 min at 80 V and a 10% separating gel for 90 min at 120 V. Proteins were then transferred to polyvinylidene difluoride membranes (Immobilon-P; EMD Millipore) using a Bio-Rad Trans-BLOT SD SEMI-DRY TRANSFER CELL system. After transferring, the membranes were blocked in 5% skimmed milk in TBS (25 mM Tris and 150 mM NaCl, pH 8.0) containing 0.05% Tween-20 (TBST) for 1 h at RT. Membranes were incubated with primary antibody in blocking solution overnight at 4°C. After washing with TBST three times (10 min each time), the membranes were incubated with an HRP-conjugated goat anti-rabbit or goat anti-mouse antibody (ZSGB-BIO) for 1–2 h at RT. Primary antibodies and dilutions were as follows: 1:400 mouse anti–Cyclin B1 (ab72; Abcam), 1:500 mouse anti–Cyclin B2 (ab18250; Abcam), 1:1,000 mouse anti–Cyclin B2 (ab185622; Abcam), 1:1,000 rabbit anti-P–lamin A/C (2026; Cell Signaling Technology), and 1:2,000–1:5,000 mouse anti-GAPDH (MB001; Bioworld). HRP levels were detected by a SuperSignal West Femto system (Thermo Fisher Scientific).

Statistical analysis

All images were analyzed with Photoshop CS5 (Adobe) and ImageJ software (National Institutes of Health). Quantitative data (mean ± SEM) were processed by Student's t test using Prism 5 (GraphPad Software) with $P < 0.05$ set for significance.

Online supplemental material

Fig. S1 shows the absence of *Ccnb1* mRNA in the oocytes and failure of embryo implantation in the *GDF9-Ccnb1*^{−/−} female mice. Fig. S2 shows the aberrant early embryonic development in the *GDF9-Ccnb1*^{−/−} mice. Fig. S3 shows the histology of ovarian sections from the *Ccnb1*[Flox/Flox] and *Ccnb1*[Flox/Flox];*GDF9-Cre* females. Fig. S4 shows the analysis of spindle shape and chromosome alignment as well as restoration of the MII arrest in the *GDF9-Ccnb1*^{−/−} oocytes. Fig. S5 shows the permanent GV arrest of *GDF9-Ccnb1*^{−/−}; *Ccnb2*^{−/−} oocytes in vitro and rescue of GVBD in *Ccnb2*^{−/−} oocytes by exogenous Cyclin B1. Video 1 shows live-cell imaging for meiosis progression in the control oocytes. Video 2 shows live-cell imaging for meiosis progression in the GDF9-Ccnb1^{−/−} oocytes. Video 3 shows live-cell imaging for nuclear import of Cyclin B2–Venus in the control oocytes. Video 4 shows live-cell imaging for nuclear import of Cyclin B2–Venus in the GDF9-Ccnb1^{−/−} oocytes.

Acknowledgments

References

Adhikari, D., and K. Liu. 2014. The regulation of maturation promoting factor during prophase I arrest and meiotic entry in mammalian oocytes. *Mol. Cell. Endocrinol.* 382:480–487. https://doi.org/10.1016/j.mce.2013.07.027

Adhikari, D., W. Zheng, Y. Shen, N. Gorre, Y. Ning, G. Halet, P. Kaldis, and K. Liu. 2012. Cdk1, but not Cdk2, is the sole Cdk that is essential and sufficient to drive resumption of meiosis in mouse oocytes. *Hum. Mol. Genet.* 21:2476–2484. https://doi.org/10.1093/hmg/dds061

Adhikari, D., M.K. Diril, K. Busayavalasa, S. Risal, S. Nakagawa, R. Lindkvist, Y. Shen, V. Coppola, L. Tessarollo, N.R. Kudo, et al. 2014. Mastl is required for timely activation of APC/C in meiosis I and Cdk1 reactivation in meiosis II. *J. Cell Biol.* 206:843–853. https://doi.org/10.1083/jcb.201406033

Borum, K. 1961. Oogenesis in the mouse. A study of the meiotic prophase. *Exp. Cell Res.* 24:495–507. https://doi.org/10.1016/0014-4827(61)90449-9

Brandeis, M., I. Rosewell, M. Carrington, T. Crompton, M.A. Jacobs, J. Kirk, J. Gannon, and T. Hunt. 1998. Cyclin B2-null mice develop normally and are fertile whereas cyclin B1-null mice die in utero. *Proc. Natl. Acad. Sci. USA.* 95:4344–4349. https://doi.org/10.1073/pnas.95.8.4344

Choi, T., F. Aoki, M. Mori, M. Yamashita, Y. Nagahama, and K. Kohmoto. 1991. Activation of p34cdc2 protein kinase activity in meiotic and mitotic cell cycles in mouse oocytes and embryos. *Development.* 113:789–795.

Clute, P., and J. Pines. 1999. Temporal and spatial control of cyclin B1 destruction in metaphase. *Nat. Cell Biol.* 1:82–87. https://doi.org/10.1038/10049

Dimova, N.V., N.A. Hathaway, B.H. Lee, D.S. Kirkpatrick, M.L. Berkowitz, S.P. Gygi, D. Finley, and R.W. King. 2012. APC/C-mediated multiple monoubiquitylation provides an alternative degradation signal for cyclin B1. *Nat. Cell Biol.* 14:168–176. https://doi.org/10.1038/ncb2425

Dorée, M., and T. Hunt. 2002. From Cdc2 to Cdk1: when did the cell cycle kinase join its cyclin partner? *J. Cell Sci.* 115:2461–2464.

Draetta, G., F. Luca, J. Westendorf, L. Brizuela, J. Ruderman, and D. Beach. 1989. Cdc2 protein kinase is complexed with both cyclin A and B: evidence for proteolytic inactivation of MPF. *Cell.* 56:829–838. https://doi.org/10.1016/0092-8674(89)90687-9

Fung, T.K., H.T. Ma, and R.Y. Poon. 2007. Specialized roles of the two mitotic cyclins in somatic cells: cyclin A as an activator of M phase-promoting factor. *Mol. Biol. Cell.* 18:1861–1873. https://doi.org/10.1091/mbc.e06-12-1092

Gautier, J., J. Minshull, M. Lohka, M. Glotzer, T. Hunt, and J.L. Maller. 1990. Cyclin is a component of maturation-promoting factor from Xenopus. *Cell.* 60:487–494. https://doi.org/10.1016/0092-8674(90)90599-A

Gui, L., and H. Homer. 2013. Hec1-dependent cyclin B2 stabilization regulates the G2-M transition and early prometaphase in mouse oocytes. *Dev. Cell.* 25:43–54. https://doi.org/10.1016/j.devcel.2013.02.008

Han, S.J., R. Chen, M.P. Paronetto, and M. Conti. 2005. Wee1B is an oocyte-specific kinase involved in the control of meiotic arrest in the mouse. *Curr. Biol.* 15:1670–1676. https://doi.org/10.1016/j.cub.2005.07.056

Han, S.J., J.P.S. Martins, Y. Yang, M.K. Kang, E.M. Daldello, and M. Conti. 2017. The Translation of Cyclin B1 and B2 is Differentially Regulated during Mouse Oocyte Reentry into the Meiotic Cell Cycle. *Sci. Rep.* 7:14077. https://doi.org/10.1038/s41598-017-13688-3

Heald, R., and F. McKeon. 1990. Mutations of phosphorylation sites in lamin A that prevent nuclear lamina disassembly in mitosis. *Cell.* 61:579–589. https://doi.org/10.1016/0092-8674(90)90470-Y

Hochegger, H., A. Klotzbücher, J. Kirk, M. Howell, K. le Guellec, K. Fletcher, T. Duncan, M. Sohail, and T. Hunt. 2001. New B-type cyclin synthesis is

required between meiosis I and II during Xenopus oocyte maturation. *Development.* 128:3795–3807.

Holt, J.E., J. Weaver, and K.T. Jones. 2010. Spatial regulation of APCcdh1-induced cyclin B1 degradation maintains G2 arrest in mouse oocytes. *Development.* 137:1297–1304. https://doi.org/10.1242/dev.047555

Holt, J.E., S.I. Lane, and K.T. Jones. 2013. Time-lapse epifluorescence imaging of expressed cRNA to cyclin B1 for studying meiosis I in mouse oocytes. *Methods Mol. Biol.* 957:91–106. https://doi.org/10.1007/978-1-62703-191-2_6

Homer, H. 2013. The APC/C in female mammalian meiosis I. *Reproduction.* 146:R61–R71. https://doi.org/10.1530/REP-13-0163

Huo, L.J., L.Z. Yu, C.G. Liang, H.Y. Fan, D.Y. Chen, and Q.Y. Sun. 2005. Cell-cycle-dependent subcellular localization of cyclin B1, phosphorylated cyclin B1 and p34cdc2 during oocyte meiotic maturation and fertilization in mouse. *Zygote.* 13:45–53. https://doi.org/10.1017/S0967199405003060

Jones, K.T. 2004. Turning it on and off: M-phase promoting factor during meiotic maturation and fertilization. *Mol. Hum. Reprod.* 10:1–5. https://doi.org/10.1093/molehr/gah009

Kanatsu-Shinohara, M., R.M. Schultz, and G.S. Kopf. 2000. Acquisition of meiotic competence in mouse oocytes: absolute amounts of p34(cdc2), cyclin B1, cdc25C, and wee1 in meiotically incompetent and competent oocytes. *Biol. Reprod.* 63:1610–1616. https://doi.org/10.1095/biolreprod63.6.1610

Kimura, H. 2013. Histone modifications for human epigenome analysis. *J. Hum. Genet.* 58:439–445. https://doi.org/10.1038/jhg.2013.66

Kubiak, J.Z. 2013. Protein kinase assays for measuring MPF and MAPK activities in mouse and rat oocytes and early embryos. *Methods Mol. Biol.* 957:77–89. https://doi.org/10.1007/978-1-62703-191-2_5

Labbé, J.C., J.P. Capony, D. Caput, J.C. Cavadore, J. Derancourt, M. Kaghad, J.M. Lelias, A. Picard, and M. Dorée. 1989. MPF from starfish oocytes at first meiotic metaphase is a heterodimer containing one molecule of cdc2 and one molecule of cyclin B. *EMBO J.* 8:3053–3058.

Lan, Z.J., X. Xu, and A.J. Cooney. 2004. Differential oocyte-specific expression of Cre recombinase activity in GDF-9-iCre, Zp3cre, and Msx2Cre transgenic mice. *Biol. Reprod.* 71:1469–1474. https://doi.org/10.1095/biolreprod.104.031757

Ledan, E., Z. Polanski, M.E. Terret, and B. Maro. 2001. Meiotic maturation of the mouse oocyte requires an equilibrium between cyclin B synthesis and degradation. *Dev. Biol.* 232:400–413. https://doi.org/10.1006/dbio.2001.0188

Li, J., A.N. Meyer, and D.J. Donoghue. 1997. Nuclear localization of cyclin B1 mediates its biological activity and is regulated by phosphorylation. *Proc. Natl. Acad. Sci. USA.* 94:502–507. https://doi.org/10.1073/pnas.94.2.502

Marangos, P., and J. Carroll. 2004. The dynamics of cyclin B1 distribution during meiosis I in mouse oocytes. *Reproduction.* 128:153–162. https://doi.org/10.1530/rep.1.00192

Murray, A.W. 2004. Recycling the cell cycle: cyclins revisited. *Cell.* 116:221–234. https://doi.org/10.1016/S0092-8674(03)01080-8

Nguyen, T.B., K. Manova, P. Capodieci, C. Lindon, S. Bottega, X.Y. Wang, J. Refik-Rogers, J. Pines, D.J. Wolgemuth, and A. Koff. 2002. Characterization and expression of mammalian cyclin b3, a prepachytene meiotic cyclin. *J. Biol. Chem.* 277:41960–41969. https://doi.org/10.1074/jbc.M203951200

Norris, R.P., L. Freudzon, M. Freudzon, A.R. Hand, L.M. Mehlmann, and L.A. Jaffe. 2007. A G(s)-linked receptor maintains meiotic arrest in mouse oocytes, but luteinizing hormone does not cause meiotic resumption by terminating receptor-G(s) signaling. *Dev. Biol.* 310:240–249. https://doi.org/10.1016/j.ydbio.2007.07.017

Peter, M., J. Nakagawa, M. Dorée, J.C. Labbé, and E.A. Nigg. 1990. In vitro disassembly of the nuclear lamina and M phase-specific phosphorylation of lamins by cdc2 kinase. *Cell.* 61:591–602. https://doi.org/10.1016/0092-8674(90)90471-P

Peter, M., C. Le Peuch, J.C. Labbé, A.N. Meyer, D.J. Donoghue, and M. Dorée. 2002. Initial activation of cyclin-B1-cdc2 kinase requires phosphorylation of cyclin B1. *EMBO Rep.* 3:551–556. https://doi.org/10.1093/embo-reports/kvf111

Polanski, Z., E. Ledan, S. Brunet, S. Louvet, M.H. Verlhac, J.Z. Kubiak, and B. Maro. 1998. Cyclin synthesis controls the progression of meiotic maturation in mouse oocytes. *Development.* 125:4989–4997.

Polański, Z., H. Homer, and J.Z. Kubiak. 2012. Cyclin B in mouse oocytes and embryos: importance for human reproduction and aneuploidy. *Results Probl. Cell Differ.* 55:69–91. https://doi.org/10.1007/978-3-642-30406-4_4

Porter, L.A., and D.J. Donoghue. 2003. Cyclin B1 and CDK1: nuclear localization and upstream regulators. *Prog. Cell Cycle Res.* 5:335–347.

Reis, A., H.Y. Chang, M. Levasseur, and K.T. Jones. 2006. APCcdh1 activity in mouse oocytes prevents entry into the first meiotic division. *Nat. Cell Biol.* 8:539–540. https://doi.org/10.1038/ncb1406

Satyanarayana, A., and P. Kaldis. 2009. Mammalian cell-cycle regulation: several Cdks, numerous cyclins and diverse compensatory mechanisms. *Oncogene.* 28:2925–2939. https://doi.org/10.1038/onc.2009.170

Solc, P., R.M. Schultz, and J. Motlik. 2010. Prophase I arrest and progression to metaphase I in mouse oocytes: comparison of resumption of meiosis and recovery from G2-arrest in somatic cells. *Mol. Hum. Reprod.* 16:654–664. https://doi.org/10.1093/molehr/gaq034

Strauss, B., A. Harrison, P.A. Coelho, K. Yata, M. Zernicka-Goetz, and J. Pines. 2018. Cyclin B1 is essential for mitosis in mouse embryos, and its nuclear export sets the time for mitosis. *J. Cell Biol.* 217:179–193. https://doi.org/10.1083/jcb.201612147

Tang, J.X., J. Li, J.M. Cheng, B. Hu, T.C. Sun, X.Y. Li, A. Batool, Z.P. Wang, X.X. Wang, S.L. Deng, et al. 2017. Requirement for CCNB1 in mouse spermatogenesis. *Cell Death Dis.* 8:e3142. https://doi.org/10.1038/cddis.2017.555

Tay, J., R. Hodgman, and J.D. Richter. 2000. The control of cyclin B1 mRNA translation during mouse oocyte maturation. *Dev. Biol.* 221:1–9. https://doi.org/10.1006/dbio.2000.9669

Thornton, B.R., and D.P. Toczyski. 2003. Securin and B-cyclin/CDK are the only essential targets of the APC. *Nat. Cell Biol.* 5:1090–1094. https://doi.org/10.1038/ncb1066

Touati, S.A., D. Cladière, L.M. Lister, I. Leontiou, J.P. Chambon, A. Rattani, F. Böttger, O. Stemmann, K. Nasmyth, M. Herbert, and K. Wassmann. 2012. Cyclin A2 is required for sister chromatid segregation, but not separase control, in mouse oocyte meiosis. *Cell Reports.* 2:1077–1087. https://doi.org/10.1016/j.celrep.2012.10.002

Ward, G.E., and M.W. Kirschner. 1990. Identification of cell cycle-regulated phosphorylation sites on nuclear lamin C. *Cell.* 61:561–577. https://doi.org/10.1016/0092-8674(90)90469-U

Worrad, D.M., P.T. Ram, and R.M. Schultz. 1994. Regulation of gene expression in the mouse oocyte and early preimplantation embryo: developmental changes in Sp1 and TATA box-binding protein, TBP. *Development.* 120:2347–2357.

Yang, J., E.S. Bardes, J.D. Moore, J. Brennan, M.A. Powers, and S. Kornbluth. 1998. Control of cyclin B1 localization through regulated binding of the nuclear export factor CRM1. *Genes Dev.* 12:2131–2143. https://doi.org/10.1101/gad.12.14.2131

Zhang, M., Y.-Q. Su, K. Sugiura, G. Xia, and J.J. Eppig. 2010. Granulosa cell ligand NPPC and its receptor NPR2 maintain meiotic arrest in mouse oocytes. *Science.* 330:366–369. https://doi.org/10.1126/science.1193573